  Bull. Chem. Soc. Jpn., 62, 1701—1709 (1989)

The IR Photochemistry of Organic Compounds. II.[1] The IR Photochemistry of Ethers: The Decomposition Patterns[2]

Tetsuro Majima,* Tadahiro Ishii,† and Shigeyoshi Arai††
The Institute of Physical and Chemical Research, Hirosawa 2-1, Wako, Saitama 351-01
†Science University of Tokyo, Kagurazaka, Shinjukuku, Tokyo 162
††Kyoto Institute of Technology, Matsugasaki, Sakyoku, Kyoto 606
(Received October 7, 1988)

The infrared multiple-photon decomposition (IRMPD) of saturated open-chain ethers has been systematically investigated with the intention of establishing their decomposition patterns. The main products in the IRMPD of ethers (**1a—f, 2**) are H_2CO, CO, H_2, and lower hydrocarbons. Acetaldehyde is additionally formed in the IRMPD of **1b** and **1d**, while acetone is formed in the IRMPD of **1d**. The observed results are explained on the basis of the decomposition of the highly vibrationally excited ethers produced in the IRMP excitation. The initial process is the homolytic cleavage of a C-O bond to yield the corresponding alkyl and alkoxyl radicals. The alkyl radicals are trapped by Br_2. Sequential splitting and addition reactions of the radicals yield primary products with a high internal energy. The primary products also decompose sequentially into stable products, in part. The sequential processes compete with collisional deactivation. Therefore, the branching ratio depends on the internal energy of the radicals and the primary products.

The infrared multiple-photon decomposition (IRMPD) of organic compounds induced by a TEA CO_2 laser irradiation has been extensively investigated, especially with relation to laser isotope separation.[3] The laser isotope separation of oxygen has received relatively little attention compared with the separation of hydrogen and carbon isotopes using Freon compounds.[4] Ethers absorb at 900—1150 cm^{-1} because of the C-O stretching vibration, and the absorption usually falls in the tunable range of a TEA CO_2 laser. Moreover, ethers have relatively high vapor pressures and a large isotopic shift of oxygen in the C-O stretching vibration among various oxygen-containing organic compounds. Therefore, ether is very suitable as the starting material in the oxygen-isotope separation by means of a TEA CO_2 laser. In fact, the ^{18}O separation in the IRMPD of dimethyl ether has been studied by Vizhin et al.[5] and Kutschke et al.[6] We have recently studied the ^{18}O separation in the IRMPD of perfluorodimethyl ether.[1] The separation selectivity was found to be 2.5 in the irradiation of 3.5 Torr (1 Torr=133.322 Pa) of perfluorodimethyl ether with the CO_2 laser radiation at 940.55 cm^{-1}, 15 $J\,cm^{-2}$, and room temperature, where the conversion was 1.4%. No other work on oxygen-isotope separation in the IRMPD of ethers has been reported, although a number of studies have been published with respect to the kinetics and dynamics in the IRMPD of ethyl vinyl ether,[7] allyl methyl ether,[8] dialkoxyalkanes,[9] 2,5-dihydrofuran,[7d] tetrahydrofuran,[10] methylated tetrahydrofuran,[11] oxetanes,[12] and tetramethyldioxetane.[13]

In order to find a suitable compound for the laser isotope separation of oxygen, it is important to study the mechanism and final products in the IRMPD of oxygen-containing compounds. In the present work we wish to report on the decomposition mechanism on the IRMPD of saturated open-chain ethers; dimethyl (**1a**), diethyl (**1b**), dipropyl (**1c**), diisopropyl (**1d**), dibutyl (**1e**), and *t*-butyl methyl (**1f**) ethers, and 1,2-dimethoxyethane (**2**). We have analyzed the stable decomposition products. Several radical intermediates are trapped by Br_2. On the basis of the results, suitable ethers for oxygen-isotope separation using a TEA CO_2 laser are suggested.

Experimental

Material. The saturated open-chain ethers (**1a—f, 2**) were purchased from Tokyo Kasei Kogyo or Nakarai Chemicals. Each ether was distilled and degassed by several freeze (−196 °C)-pump-thaw cycles. Gas-chromatographic analyses of the ethers showed their purities to be over 99.5% and revealed no trace of possible decomposition products. All the other reagents and chemicals were commercially available and were used after distillation and degassing.

Apparatus and Procedure. A schematic diagram of the experimental set-up is shown in Fig. 1. A conventional glass vacuum system with an oil diffusion pump was used for the gas handling. The pressures were measured with a MKS Baratron-type 222B (0—10 Torr) gauge. The irradiation cell was a cross-type Pyrex tube equipped with four KBr windows (5 mm thick). The dimensions were 2 cm in diameter, 10 cm in the direction of the laser irradiation, and 5 cm in the direction of the infrared spectroscopic measurements. The IR absorption spectra were measured before and after irradiation by using a Japan Spectroscopic A-102 spectrophotometer.

A Lumonics 103-2 TEA (transversely excited atmospheric) CO_2 laser was operated using a mixture of CO_2 and He as flowing gases at a repetition rate of 0.7 Hz. The pulse width was about 80 ns FWHM without tailing. The laser lines were checked with an Optical Engineering CO_2 spectrum analyzer. The laser beam was passed through an aperture 1.0 cm in diameter and then tightly focused into the center of the cell using a BaF_2 lens with a focal length of 7.5 cm. The incident laser energy was attenuated by inserting one or more polyethylene films perpendicular to the beam path, and it was calibrated with a Scientech 364 disk calo-

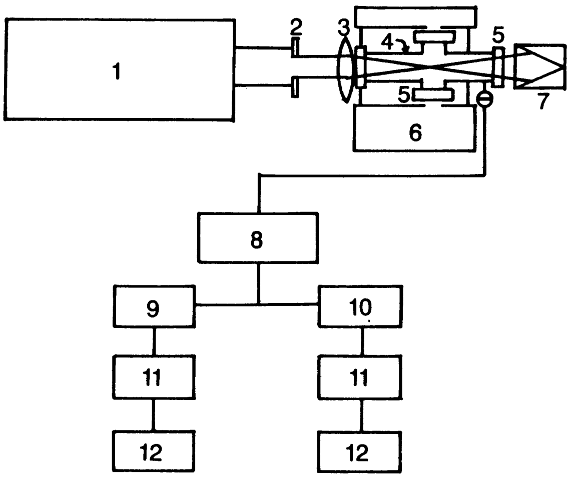

Fig. 1. Schematic diagram of the experimental set-up. 1: TEA CO_2 laser, 2: aperture, 3: BaF_2 lens, 4: reaction cell, 5: KBr window, 6: IR spectrometer, 7: power meter, 8: Toepler pump, 9: condensable gas at −196 °C, 10: non-condensable gas at −196 °C, 11: gas chromatograph, 12: mass spectrometer.

rimeter. The laser fluence at the focus corresponds to the incident pulse energy divided by the focus area (7.1×10^{-4} cm^2), which can be calculated from the aperture diameter, the focal length, and the beam divergence of 2 mrad.

Analysis. After the IR spectral measurements, sample mixtures were separated into two components, condensable gases and non-condensable gases, at −196 °C (H_2, CO, and CH_4) by using a Toepler pump. Both components were analyzed with gas chromatography (Shimadzu GC-7A, Hitachi 163, or Gasukuro Kogyo 373 gas chromatographs) using a flame-ionization or thermal-conductivity detector. Each gas chromatograph was connected to a sample injector and a integration recorder (Shimadzu Chromatopac C-R1B, Hewlett-Packard Integrator 3380, or SIC Chromatocorder 11). The lower hydrocarbons were analyzed on a Porapak Q 50/80 mesh column. The conditions were as follows: column length and diameter ($L\times\phi$), 6 m×3 mm; column temperature (CT), 150 °C; injection temperature (IT), 170 °C; detector (D), flame-ionization detector at 150 °C; carrier gas (CG), N_2; flow rate (FR), 50 $cm^3\,min^{-1}$. The lower hydrocarbons were also analyzed on a Sebaconitrile 10%-Uniport C 60/80 mesh column ($L\times\phi$, 10 m×3 mm; CT, 30 °C; IT, 50 °C; D, flame-ionization detector at 50 °C; CG, N_2; FR, 20 cm^3 min^{-1}). The ethers and bromine-containing compounds were analyzed on a PEG-20 M column ($L\times\phi$, 7 m×3 mm; CT, 90 °C; IT, 100 °C; D, flame-ionization detector at 100 °C; CG, N_2; FR, 30 cm^3 min^{-1}). The aldehydes were analyzed on a TSR-1 10%-Flusin T 30/60 mesh column ($L\times\phi$, 2 m×3 mm; CT, 100 °C; IT, 120 °C, D; thermal-conductivity detector at 100 °C; CG, He; FR, 27 cm^3 min^{-1}). The non-condensable gases (H_2, CO, CH_4) were analyzed on an Unibeads C 80/10 mesh column ($L\times\phi$, 3 m×3 mm; CT, 40—100 °C; IT, 100 °C; D, thermal-conductivity detector at 100 °C; CG, He; FR, 50 cm^3 min^{-1}).

A typical chromatogram of each irradiated ether showed that the peaks were fully resolved and reproducible. Standard mixtures were prepared to calibrate the gas chromatograms. The identification of the products by gas-chromatograph was based on a comparison of the product-retention times with those of the standards. The quantitative amounts of products and reactants were calibarted using gas-chromatographic sensitivity factors which had been determined by measuring the peak areas of pure standards on a integration recorder.

A mass spectrometer (Japan Electron Optics JMS-01SG) and GC-MS system (a NEVA TE-150 mass spectrometer combined with a Shimadzu GC-7A gas chromatograph) were also used to identify products, especially bromine-containing products, in the IRMPD of ether-Br_2 mixtures.

Results

The irradiation of ethers at 3.0 Torr with TEA CO_2 laser pulses caused the IRMPD to yield various products, as is shown in Tables 1—4. The laser line was tuned to the frequency coinciding with the strong absorption of the ether. The numbers of laser pulses were 100—500, and the conversions were 10—20%. The absorption coefficient (ε) of ether at the laser line changes from ether to ether in the range of 1.0×10^{-3}—7.5×10^{-2} $Torr^{-1}\,cm^{-1}$, while the decomposition yield ($Y_d=(1-P/P_0)/$(number of laser pulses)) varies slightly in the range of 3.7×10^{-4}—8.0×10^{-4} $pulse^{-1}$ (Table 1), where P_0 (=3.0 Torr) and P are the ether pressures before and after irradiation respectively.

The main decomposition products were H_2, CO,

Table 1. Irradiation Parameters in the IRMPD of **1a—f** and **2**

Ether	$\lambda^{a)}$ cm^{-1}	$\varepsilon^{b)}\times10^3$ $Torr^{-1}\,cm^{-1}$	$E_p^{c)}$ $J\,pulse^{-1}$	$F^{d)}$ $J\,cm^{-2}$
1a	1079.90	70.6	0.193	271
1b	1078.59	2.45	0.253	356
1c	1085.75	1.92	0.198	279
1d	1035.74	3.96	0.186	262
1e	1046.85	1.02	0.212	299
1f	1084.64	75.0	0.176	248
2	1039.37	1.23	0.203	286

a) Laser wavenumber. b)Absorption coefficient at the laser wavenumber. c) Incident pulse energy. d) Laser fluence at the focus.

Table 2. Product Yields in the IRMPD of **1a—f** and **2**

Ether	$Y_d^{a)}\times10^4$	$Y^{b)}\times10^4$ ($pulse^{-1}$)			$MB^{c)}$
	$pulse^{-1}$	H_2	O-compnd.[d)]	Hydrocarbons	%
1a	7.87	4.10	5.50	2.07	70
1b	3.97	1.71	2.22	4.77	60
1c	6.83	3.80	4.67	4.93	68
1d	3.77	3.08	3.21	3.93	85
1e	5.43	2.00	3.23	19.3	60
1f	7.40	9.93	4.57	6.53	62
2	5.87	2.08	8.02	10.5	70

a) Decomposition yield of ether. b) Yield of product. c) Material balance based on oxygen atom: MB=($\sum$ (oxygen-containing products)/(consumed **1**))×100 for **1** and MB=($\sum$(oxygen-containing products)/2 (consumed **2**))×100 for **2**. d) Oxygen-containing products.

Table 3. Relative Yields of Oxygen-Containing Products

Product	Relative yields of product[a)](%)						
	1a	1b	1c	1d	1e	1f	2
CO	37	25	35	34	23	15	17
H_2CO	63	66	65	8	77	85	83
CH_3CHO	0	9	0	54	0	0	0
CH_3COCH_3	0	0	0	4	0	0	0

a) Relative yield of product to total yield of oxygen-containing products.

Table 4. Relative Yields of Hydrocarbon Products

Product	Relative yields of product[a)] (%)						
	1a	1b	1c	1d	1e	1f	2
CH_4	14	38	8	12	12	0	18
C_2H_6	57	17	16	14	13	14	51
C_2H_4	18	27	6	13	49	6	30
C_2H_2	2	4	0.1	2	0.1	0.3	0.6
C_3H_8	6	14	15	1	12	0.3	0.6
C_3H_6	1	0	38	52	3	2	0.1
CH_3CCH	0	0	0	1	0	0	0
CH_2CCH_2	0	0	0	1	0	2	0
n-C_4H_{10}	3	0	11	0	3	0	0
Δ^1-C_4H_8	0	1	2	3	7	0	0.3
i-C_4H_8	0	0	0	0	0	75	0
$\Delta^{1,3}$-C_4H_6	0	0	0	0.3	0	0	0
n-C_5H_{12}	0	0	3	0	1	0	0

a) Relative yield of product to total yield of hydrocarbon products.

H_2CO, and lower hydrocarbons. Additionally, acetaldehyde (CH_3CHO) and acetone (CH_3COCH_3) were formed in the IRMPD of **1b** and **1d** and of **1d**. The yields (Y=(pressure of product)/(P_0×(number of laser pulses)) of H_2, oxygen-containing compounds, and hydrocarbons are shown in Tables 2 and 3. Neither alcohol nor aldehyde containing more than three carbon atoms was detected. The material balance based on the oxygen atoms were very good—60—85%, as is shown in Table 2. The material balance is defined as {∑(pressures of oxygen-containing products)/(consumed ether) (number of oxygen atoms in ether)}×100%. Thus, the oxygen atoms in the decomposed ether were found mostly in CO, H_2CO, or CH_3CHO.

On the other hand, the distributions of the hydrocarbons were dependent on the ethers. The yield of a hydrocarbon relative to the total yield of hydrocarbons is presented for each ether in Table 4. The main hydrocarbons reflected the structures of the alkyl groups of the ethers: ethane (C_2H_6) and ethylene (C_2H_4) for **1a**, **1b**, and **2**; propylene (C_3H_6) for **1c** and **1d**; C_2H_4 for **1e**; isobutene for **1f**.

The value of Y_d increased with the increase in the laser fluence at the focus (F); Y_d was proportional to $F^{1.3-1.7}$. In addition, the product distributions also changed with F. The relationships between Y_d and F and the product distribution vs. F in the IRMPD of **1a**

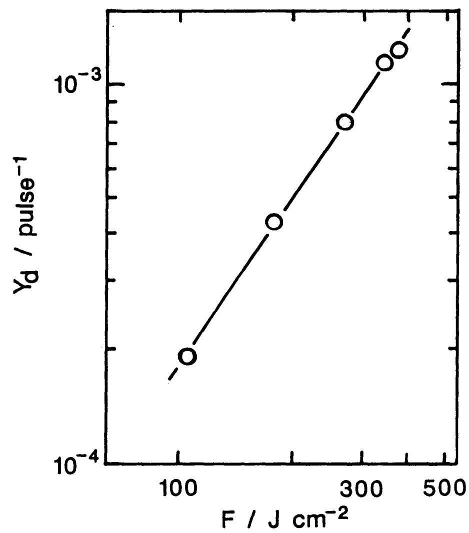

Fig. 2. Log-log plot of the decomposition yield (Y_d) vs. laser fluence at the focus (F) in the IRMPD of **1a** of 3.0 Torr.

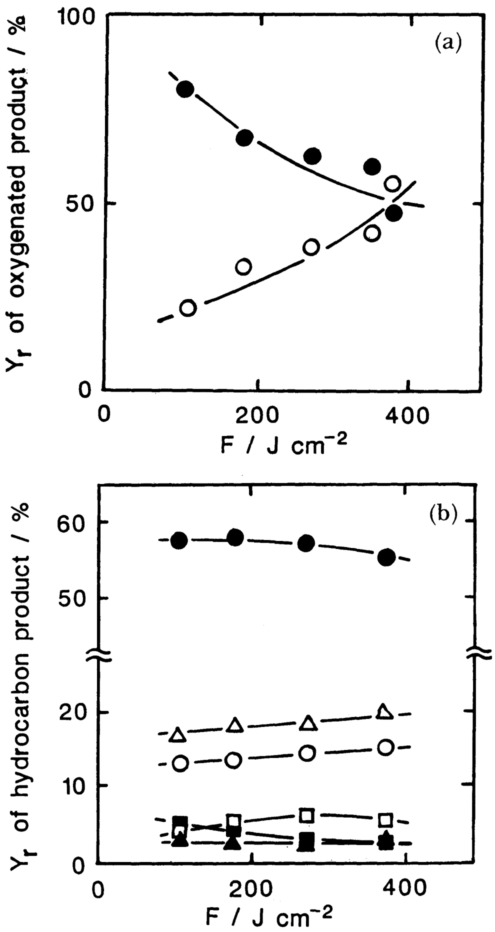

Fig. 3. Effects of F on the distribution (a) of oxygen-containing products: CO (○) and H_2CO (●) and (b) of hydrocarbon products: CH_4 (○), C_2H_6 (●), C_2H_4 (△), C_2H_2 (▲), C_3H_8 (□), and n-C_4H_{10} (■) in the IRMPD of **1a** at 3.0 Torr. The ordinate, Y_r, indicates relative yields of an oxygen-containing product and of a hydrocarbon product to the total yields of oxygen-containing products and of hydrocarbon products respectively.

Table 5. Relative Yields of Bromine-Containing Products in the IRMPD of Ether-Br_2 Mixtures

Ether	Relative yields of bromine-containing product[a] (%)					
	CH_3Br	CH_2Br_2	C_2H_5Br	$C_2H_4Br_2$	C_3H_7Br	t-C_4H_9Br
1a	95	5	0	0	0	0
1b	46	1	54	2	0	0
1c	23	2	10	1	64	0
1f	12	0	0	0	0	88

a) Relative yield of product to total yield of bromine-containing products.

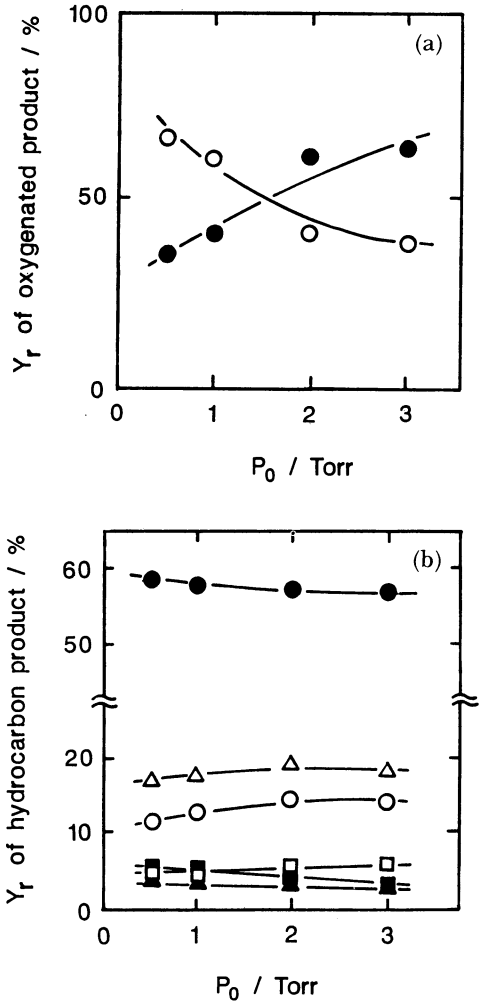

Fig. 4. Effects of P_0 on the distribution (a) of oxygen-containing products: CO (○) and H_2CO (●) and (b) of hydrocarbon products: CH_4 (○), C_2H_6 (●), C_2H_4 (△), C_2H_2 (▲), C_3H_8 (□), and n-C_4H_{10} (■) at F=271 J cm^{-2} in the IRMPD of **1a**.

are shown in Figs. 2 and 3 respectively. With the increase in F, H_2CO decreased, while CO increased in its relative yield, as is shown in Fig. 3a. On the other hand, the distribution of hydrocarbon products was hardly affected by F, as is shown in Fig. 3b.

The pressure dependence on the product distribution was examined in the range of 0.5—3.0 Torr at the same F in the IRMPD of **1a**. With the increase in the P_0 of **1a**, the relative yield of H_2CO increased, while that of CO decreased, as is shown in Fig. 4a. On the other hand, the distribution of hydrocarbon products did not significantly change with the P_0, as is shown in Fig. 4b.

When 3.0 Torr of ether was irradiated in the presence of 3.0 Torr of Br_2, bromine-containing compounds were formed with the decreases in the decomposition products (Table 5). Methyl bromide (CH_3Br) was the main product in the IRMPD of the **1a**-Br_2 mixture. A small amount of dibromomethane (CH_2Br_2) was also formed. Both CH_3Br and ethyl bromide (C_2H_5Br) in the ratio of 46 : 54 were formed in the IRMPD of the **1b**-Br_2 mixture, while t-butyl bromide (t-C_4H_9Br) and CH_3Br in the ratio of 88 : 12 were formed in the IRMPD of the **1f**-Br_2 mixture.

Discussion

Infrared multiple-photon excitation is different from UV excitation into an electronically excited state or thermal excitation, although there are similarities among the products formed in the IRMPD, vacuum-UV photolysis,[14] and thermolysis.[14a,15] The irradiation of ether using a TEA CO_2 laser yields highly vibrationally excited ether, E*, through IRMP excitation, with the asterisk denoting vibrational excitation.[3,4,16,17] The distribution of vibrational energy is usually approximated by the Boltzmann law.[16] Thus, the IRMPD can be well-explained by the statistical unimolecular decomposition according to the RRKM theory.[17,18] At high fluences, however, most of the molecules absorb more energy than is required for the dissociation of a bond.

Generally the weakest bond is broken in highly vibrationally excited molecules.[17] The cleavage of a C-O bond is obviously the lowest dissociation channel; the dissociation energy (E_{diss}) has been reported to be 81 kcal mol^{-1} in **1a**. A decomposition mechanism involving the initial cleavage of the C-O bond has been proposed in the IRMPD of **1a**.[5,6] Vacuum-UV photolysis and conventional thermolysis of ether in a vapor phase have also been explained on the basis of the initial cleavage of a C-O bond. The product distributions in the IRMPD of ethers are similar to those in UV-photolysis and thermolysis. Therefore, it is strongly suggested that the initial process in E* is the homolytic cleavage of the C-O bond, yielding alkyl (R·) and alkoxyl radicals (R′O·) according to Eq. 1 (all the products are postulated to arise from the radicals):

$$\text{R-O-R}' \xrightarrow{nh\nu} \text{R}\cdot + \cdot\text{OR}' \quad (1)$$

1a—f, **2** (R, R′=alkyl)

The energy absorbed by ethers (E_{abs}) must be as large as the E_{diss} of the C–O bond in ethers. Since the E_{abs} of decomposing ether is generally much larger than the E_{diss} at high fluences, R· and R′O· are formed with a high internal energy and decompose into the primary products either sequentially or via secondary IRMPD. The primary products are also formed with a high internal energy and, therefore, decompose into stable products or are stabilized via collisional deactivation. It has previously been pointed out that the sequential decomposition or secondary IRMPD of radical intermediates and primary products with a high internal energy occurs favorably in the IRMPD of organic compounds, even if their 1←0 absorptions are not resonant with the laser radiation.[10,19]

In the IRMPD of ethers, radicals are formed spatially at a higher concentration by using a tightly focused laser beam. The relationship of $Y_d \propto F^{1.3-1.7}$ (shown in Fig. 2) means that the decomposition yield in the IRMPD of **1** and **2** approximately follows the 1.5-power rule; the fluence is much higher than the threshold one, and all the molecules in the region around a focal point decompose completely and yield radicals at high concentrations. Therefore, radical-radical reactions occur, while reactions between radicals and starting ethers are not involved. In fact, all the products in the IRMPD of ethers were either decomposition fragments or radical-radical reaction products. There were no detectable products originating from the reactions between radicals and ethers.

1a. From the distribution of decomposition fragments, the reaction processes of the radicals are considered to be as follows. The cleavage of the C–O bond in **1a*** gives primarily a methyl radical ($CH_3\cdot$) and a methoxyl radical ($CH_3O\cdot$). The radicals then react each other via coupling and disproportionation (Scheme 1).

Since methanol was not detected, disproportionation between two $CH_3O\cdot$ or H-abstraction from **1a** by $CH_3O\cdot$ did not occur. Thus, $CH_3O\cdot$ reacts with $CH_3\cdot$ via H-abstraction to yield H_2CO and CH_4 or decomposes into H_2CO and H. The activation energy (E_a) for the latter process has been reported to be 30 kcal mol^{-1}.[20] When the E_{diss} of decomposing **1a*** is higher than the summation of E_{diss} for the C–O bond plus E_a for the decomposition of $CH_3O\cdot$ into H $+H_2CO$ (i.e., $E_{abs} > E_{diss} + E_a = 111$ kcal mol^{-1}), the internal energy of $CH_3O\cdot$ is so high that $CH_3O\cdot$ decomposes sequentially. Alternatively, there is a possibility that the secondary IRMPD of $CH_3O\cdot$ occurs within a laser pulse, if $CH_3O\cdot$ is formed in highly excited vibrational states and absorbs further laser radiation. The primary product H_2CO is probably formed with a high internal energy. Therefore, $H_2CO^\dagger$ may, at least in part, decompose sequentially or via the secondary IRMPD into $CO+H_2$. (The dagger denotes a high internal energy.) This decomposition is strongly suggested because the heat of reaction is only 1.3 kcal mol^{-1}.[21] Alternatively the decomposition of $H_2CO^\dagger$ into HCO+H may occur to yield CO as the final product. It is not clear whether the molecular pathway or the radical pathway is involved in the sequential decomposition of $H_2CO^\dagger$. However, CO is the final product in both pathways.

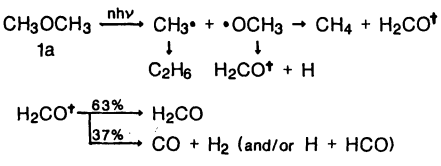

Scheme 1.

The sequential decomposition of $H_2CO^\dagger$ competes with the collisional deactivation process to give H_2CO in the ground state. The ratio of the sequential decomposition of $H_2CO^\dagger$ to the deactivation process depends on the internal energy and can be estimated from the ratio of CO to H_2CO. At higher F values, a faster IRMP excitation leads to higher internal energies of **1a*** and $H_2CO^\dagger$ and accelerates the sequential decomposition. At lower P_0 values, the collisional deactivation decreases, while the sequential decomposition increases. In fact, we observed that the ratio increased from 20 to 50% with the increase in F from 105 to 375 J cm^{-2} (Fig. 3a) and that the ratio increased from 37 to 65% with the decrease in P_0 from 3 to 0.5 Torr (Fig. 4a).

Since $CH_3\cdot$ is also produced with a high internal energy, such primary products as CH_4 and C_2H_6 are probably formed with high internal energies. However, the primary hydrocarbon products are mostly stabilized by the collisional deactivation processes because of the higher E_a values for the cleavage of C–H and C–C bonds, 102 and 85 kcal mol^{-1} respectively[22] in CH_4 and C_2H_6 compared with those in $H_2CO^\dagger$.[21] This is consistent with the absence of any effect of F and P_0 on the distribution of hydrocarbon products in the range of 105—375 J cm^{-2} of F (Fig. 3b) and in the range of 0.5—3 Torr (Fig. 4b). The formation of C_2H_4, C_2H_2, C_3H_8, and other hydrocarbons is explained by the following sequence of reactions (Eqs. 2—12), which are all involved in high-temperature chemistry:[23]

$$CH_3\cdot + CH_3\cdot \rightarrow C_2H_6 \quad (2)$$

$$CH_3\cdot + C_2H_6 \rightarrow CH_4 + C_2H_5\cdot \quad (3)$$

$$C_2H_5\cdot \rightarrow C_2H_4 + H \quad (4)$$

$$H + C_2H_6 \rightarrow H_2 + C_2H_5\cdot \quad (5)$$

$$CH_3\cdot + C_2H_5\cdot \rightarrow C_3H_8 \quad (6)$$

$$CH_3\cdot + C_2H_5\cdot \rightarrow CH_4 + C_2H_4 \tag{7}$$

$$H + C_2H_4 \rightarrow H_2 + C_2H_3 \tag{8}$$

$$CH_3\cdot + C_2H_4 \rightarrow CH_4 + C_2H_3 \tag{9}$$

$$C_2H_3 \rightarrow H + C_2H_2 \tag{10}$$

$$H + C_2H_5\cdot \rightarrow 2CH_3\cdot \tag{11}$$

$$H + C_2H_3 \rightarrow C_2H_4 \tag{12}$$

According to Scheme 1, the total yield of oxygen-containing products is expected to be equal to the total yield of C_n hydrocarbon products multiplied by n. The actual ratio of the two yields was, however, 1 : 0.74; several oxygen-containing products have not been detected. The value of $[CO]/([CO]+[H_2CO])=0.37$ means that $H_2CO^\dagger$ decomposes into $CO+H_2$ in a 37% yield and is stabilized into H_2CO in a 63% yield. The ratio of $[H_2]/[CO]=2.0$ suggests that H_2 is formed not only via the decomposition of $H_2CO^\dagger$ but also via other reactions of the alkyl radicals.

Similar mechanisms involving the sequential decomposition of primary products into final products have been proposed in the IRMPD of organic molecules.[10,19] The sequential decomposition process competes with the collisional deactivation process and, therefore, occurs more easily with smaller E_a and larger E_{abs} values. The sequential (and/or secondary) process distinguishes the IRMPD from thermolysis and shock-wave decomposition, although the sequential decomposition process sometimes occurs in thermolysis at extremely high temperatures.[24]

1b. A similar mechanism is proposed for the IRMPD of **1b** (Scheme 2). The initial cleavage of the C–O bond yields $C_2H_5\cdot$ and $C_2H_5O\cdot$. The disproportionation of $C_2H_5\cdot$ gives C_2H_4 and C_2H_6. The β-fission of $C_2H_5O\cdot$ yields $H_2CO^\dagger$ and $CH_3\cdot$, while $C_2H_5O\cdot$ decomposes partly into $CH_3CHO^\dagger$ by the splitting of H. The energy requirement for the cleavage of the C–C bond is considerably less in the decomposition of $C_2H_5O\cdot$.[25] Therefore, the cleavage of the C–C bond must occur favorably; the yield of $H_2CO^\dagger$ is then higher than that of $CH_3CHO^\dagger$.

The sequential decomposition of $CH_3CHO^\dagger$ with a high internal energy yields CH_4+CO (and/or $CH_3\cdot$ $+HCO$) in a manner similar to that found with $H_2CO^\dagger$ (Scheme 1). Even if $CH_3\cdot$ and HCO are formed, CH_4, C_2H_6, and CO are mainly formed. Therefore, CH_4 and CO are the final products in the sequential decomposition of $CH_3CHO^\dagger$.

On the basis of the value of [CO]/[oxygen-containing products]=0.25 and the value of $[CH_3CHO]/([H_2CO]+[CH_3CHO])=0.12$, the branching ratios in the decomposition of $C_2H_5O\cdot$ and in the decomposition of $H_2CO^\dagger$ and $CH_3CHO^\dagger$ can be roughly estimated. When x, y, and z denote the ratios of the decomposition of $C_2H_5O\cdot$ into $H_2CO^\dagger$ plus $CH_3\cdot$, and those of the deactivations of $H_2CO^\dagger$ into H_2CO and of $CH_3CHO^\dagger$ into CH_3CHO, respectively, Eqs. 13 and 14 are derived (see Scheme 2):

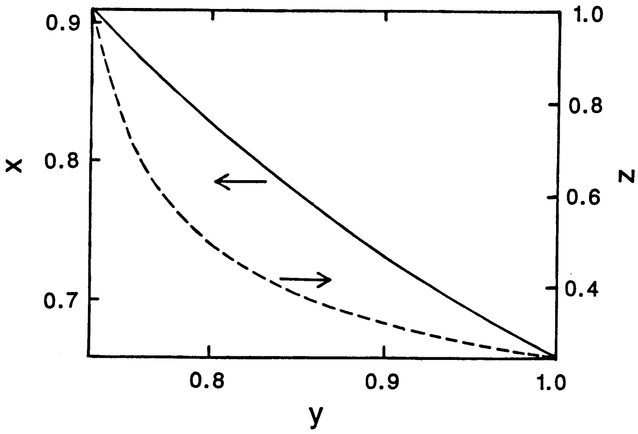

Fig. 5. Relationships of x, y, and z. Values of x and z are calculated as a function of y. For x, y, and z, see the text.

$$x=1/(1+0.136y/z) \tag{13}$$

$$z=1/(11.1-7.33/y) \tag{14}$$

The values of x and z are calculated as a function of y, as is shown in Fig. 5.

A higher branching ratio of the decomposition of $C_2H_5O\cdot$ into $H_2CO^\dagger$ and $CH_3\cdot$ than that into $CH_3CHO^\dagger$ and H can easily be expected from the energy difference between the cleavages of the β C–C and β C–H bonds in $C_2H_5O\cdot$. When the branching ratios of the sequential decomposition to collisional deactivation are equivalent in $H_2CO^\dagger$ and $CH_3CHO^\dagger$, one can obtain $y=z=0.75$ and $x=0.88$. However, the sequential decomposition is considered to be much more favored in $CH_3CHO^\dagger$ than in $H_2CO^\dagger$. It is expected that a small fragment H does not remove the excess energy, while the excess energy remains mainly in a large fragment. Therefore, $CH_3CHO^\dagger$ has a higher internal energy and decomposes sequentially in a higher yield than does $H_2CO^\dagger$. This means that $y>0.75$ and $z<0.75$ and that, therefore, $x<0.88$. If y is close to unity, one can obtain $x=0.67$ and $z=$ 0.27. The ranges of x, y, and z are determined to be as shown in Scheme 2.

The formation of hydrocarbon products is also explained by these reactions (Eqs. 2—12) and similar reactions involving $C_2H_5\cdot$. Since a considerable

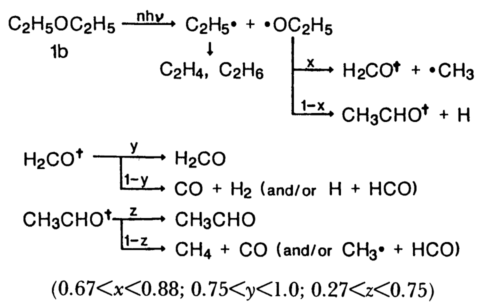

($0.67<x<0.88$; $0.75<y<1.0$; $0.27<z<0.75$)

Scheme 2.

amount of propane (C_3H_8) is formed, the coupling reaction between $C_2H_5\cdot$ and $CH_3\cdot$ (Eq. 6) is particularly important.

1c and 1e. The cleavage of the C–O bond produces propyl (n-$C_3H_7\cdot$) and propoxyl radicals (n-$C_3H_7O\cdot$) in the IRMPD of **1c**, and butyl (n-$C_4H_9\cdot$) and butoxyl radicals (n-$C_4H_9O\cdot$) in the IRMPD of **1e** (Scheme 3).

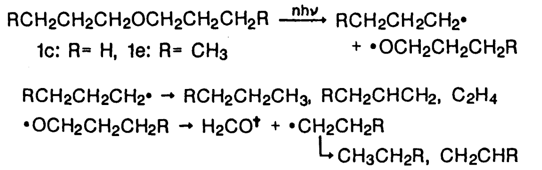

Scheme 3.

n-$C_3H_7\cdot$ disproportionates into C_3H_8 and C_3H_6, while n-$C_4H_9\cdot$ decomposes into C_2H_4 and $C_2H_5\cdot$ via β-fission. Since CO and H_2CO were the only detectable products containing an oxygen atom, it can be said that the cleavage of the β C–C bond in n-$C_3H_7O\cdot$ and n-$C_4H_9O\cdot$ occurs predominantly to form $H_2CO^\dagger$+$C_2H_5\cdot$ and $H_2CO^\dagger$+n-$C_3H_7\cdot$ respectively. It is well-established that the elimination of an alkyl redical from alkoxyl radicals occurs much faster than that of a hydrogen atom in thermolyses and UV photolyses.[25,26]

1d. The isopropoxyl radical (i-$C_3H_7O\cdot$) formed in the IRMPD of **1d** decomposes mostly into $CH_3CHO^\dagger$+$CH_3\cdot$ and slightly into $CH_3COCH_3^\dagger$+H (Scheme 4). The estimation of the branching ratio

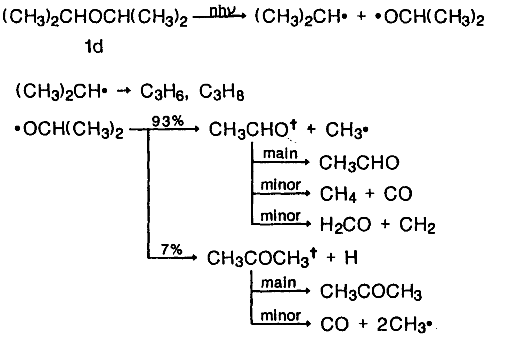

Scheme 4.

between the two processes from the value of $[CH_3COCH_3]/([CH_3COCH_3]+[CH_3CHO])$ shows that the latter process produces only in a 7% yield. It is assumed in the estimation that the branching ratios of stabilization and decomposition for $CH_3CHO^\dagger$ and $CH_3COCH_3^\dagger$ are similar to each other. The selective decomposition of i-$C_3H_7O\cdot$ into CH_3CHO+$CH_3\cdot$ is due to the smaller value of E_a=11.8 kcal mol^{-1}.[27] Additionally, H_2CO is formed in an 8% yield relative to the total yield of the oxygen-containing products. Therefore, $CH_3CHO^\dagger$ is mainly deactivated into CH_3CHO and slightly decomposes into CH_4+CO and H_2CO+CH_2. Similarly, $CH_3COCH_3^\dagger$ is mostly stabilized to CH_3COCH_3 and partly decomposes into $2CH_3\cdot$+CO, probably via the secondary IRMPD.

1f. In contrast to **1a—d**, **1f** does not have a symmetric structure; rather it has two different alkyl groups separated by an oxygen atom. Therefore, it is interesting to see which C–O bond cleaves initially in the IRMPD of **1f**. The oxygen-containing products are CO and H_2CO, while isobutene (i-C_4H_8) is formed in a 75% yield relative to the total yield of hydrocarbon products. Thus, the cleavage of the C–O bond of a t-butyl group occurs selectively to form the t-butyl radical ($(CH_3)_3C\cdot$) and $CH_3O\cdot$ (Scheme 5). The

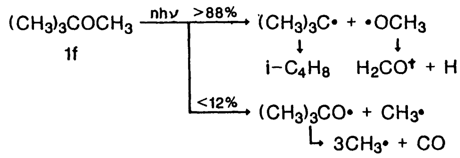

Scheme 5.

minor cleavage of the other C–O bond gives the t-butoxyl radical (t-$C_4H_9O\cdot$) and $CH_3\cdot$. Since neither CH_3CHO nor CH_3COCH_3 was detected, t-$C_4H_9O\cdot$ may be scarcely formed at all, or it may decompose into small fragments. If i-C_4H_8 is formed in the main channel and C_2 hydrocarbons are formed from the $CH_3\cdot$ produced in the minor channel, the selectivity for the main cleavage can be estimated to be 88% from $[i\text{-}C_4H_8]/([i\text{-}C_4H_8]+0.5\times[C_2 \text{ hydrocarbons}])=0.88$. This value probably corresponds to the lower limit, because $CH_3\cdot$ may be produced from t-$C_4H_9O\cdot$. The selectivity is due to the considerably smaller value of E_{diss} for a t-C_4H_9–O bond (ca. 60 kcal mol^{-1})[28] than that for a CH_3–O bond (81 kcal mol^{-1}).[17]

2. On the other hand, the cleavages of two different C–O bonds are involved in the IRMPD of **2**. One process gives $CH_3OCH_2CH_2\cdot$+$CH_3O\cdot$, while the other gives $CH_3OCH_2CH_2\cdot$+$CH_3\cdot$, as is shown in Scheme 6. Both $CH_3OCH_2CH_2\cdot$ and $CH_3OCH_2CH_2O\cdot$ de-

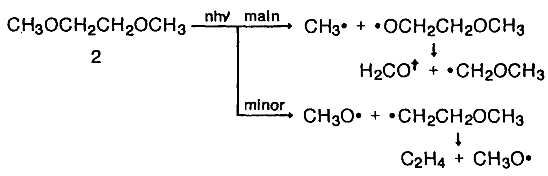

Scheme 6.

compose mainly via β-fission. Since C_2H_6 is formed in a higher yield than is C_2H_4 (1.7 : 1), the C–O cleavage to form $CH_3\cdot$ occurs more preferentially than that to form $CH_3O\cdot$. However, the selectivity of the cleavage is small because of the similar values of E_{diss} for the two C–O cleavages.

On the basis of the distributions of the products in the IRMPD of open-chain ethers, the decomposition mechanisms discussed above may be summarized as follows. The homolytic cleavage of the C-O bond in E* occurs primarily to form alkyl and alkoxyl radicals. Since radicals are formed with high internal energies, they further decompose and rearrange sequentially or via the secondary IRMPD. The primary products are mainly formed through β-fission. Since the primary products are also considered to be formed with high internal energies, further decomposition into the stable products occurs, at least in part. The stable products are mostly decomposition fragments, plus a few radical-radical reaction products. No product from any reactions between redicals and ethers was detected. These results are attributable to either the properties of E* in the high vibrational states or to the geometrical specificities of the reaction field in the focused laser beam.

It has been demonstrated that Br_2 is an efficient scavenger of radicals, but it does not initiate chain reactions.[29] The formation of CH_3Br has already been reported in the IRMPD of a mixture of **1a** and Br_2 by Vizhin et al.[5] We have also studied the IRMPD of mixtures of several ethers and Br_2 in order to elucidate the radical intermediates (Table 5). The predominant formation of CH_3Br in the IRMPD of mixture of **1a** and Br_2 clearly shows the intermediary of $CH_3\cdot$ (Scheme 1). The formation of a small amount of CH_2Br_2 suggests that CH_2 is trapped by Br_2. Comparable amounts of CH_3Br and C_2H_5Br were formed in the IRMPD of a mixture of **1b** and Br_2. This suggests a comparable formation of $CH_3\cdot$ and $C_2H_5\cdot$. Therefore, $C_2H_5O\cdot$ splits mainly into $H_2CO^{\dagger}+CH_3\cdot$ (Scheme 2). The ratio of $[t\text{-}C_4H_9Br]:[CH_3Br]=88:12$ was obtained in the IRMPD of a mixture of **1f** and Br_2. This shows that the cleavage of a $t\text{-}C_4H_9\text{-}O$ bond occurs selectively in an 88% yield to produce $t\text{-}C_4H_9\cdot+\cdot OCH_3$. The value of the selectivity is equal to the value estimated from the product ratio of $[i\text{-}C_4H_8]/([i\text{-}C_4H_8]+0.5\times[C_2 \text{ hydrocarbons}])=0.88$ (Scheme 5). On the other hand, no bromine-containing compounds of alkoxyl radicals were observed because of the instability of an O–Br bond, even at room temperature.[30]

We have discussed the mechanism of the IRMPD of ethers on the basis of the distribution of the products. However, it has been pointed out that the distribution of the products is generally changed by variations in the irradiation parameters in the IRMPD of organic compounds.[3,4] The sequential processes and the secondary IRMPD of the intermediates compete with collisional deactivation. The branching ratio depends on the internal energies of the radicals and the primary products. Therefore, the branching ratios obtained in the present study are limited to the irradiation conditions of the present experiment. Other competitive processes might produce lower yields under different conditions. However, the main decomposition products are always the same, as is shown in Schemes 1—6, because the initial process is always the cleavage of a C–O bond.

There is a notable finding with respect to the values of ε and Y_d in Tables 1 and 2. **1a** and **1f** have larger ε and Y_d values compared with the other ethers. This result suggests that the $1\leftarrow0$ absorption is very important in IRMP excitation. On the other hand, **1c** has a relatively smaller ε value but a larger Y_d value. The dissociation energy of the bond cleavage and the activation energy of a sequential reaction process probably change with **1a—f** and **2**. Therefore, the decomposition efficiency is dependent not only on the $1\leftarrow0$ absorption, but also on the dissociation and the activation energies for the reaction processes.

Ethers have several advantages as starting materials for the oxygen-isotope separation by use of a TEA CO_2 laser. Firstly, the initial step is the cleavage of a C–O bond. Secondly, the resulting alkoxyl radicals sequentially split into H_2CO or CH_3CHO, which further decompose partly into CO as a stable oxygen-containing product. Since no reactions of alkoxyl radicals with ethers are involved, the isotope selectivity in the cleavage of a C–O bond is predicted to be retained even in the final product, CO. Although the sequential decomposition processes of alkoxyl radicals complicate hydrocarbon products, CO is always the main product among the oxygen-containing products.

When ^{18}O-ether decomposes into alkyl and alkoxyl racicals through selective IRMP excitation, the ^{18}O-alkoxyl radical decomposes sequentially into CO and also reacts partly with ^{16}O-ether in the reaction volume. The bimolecular reactions, together with the vibrational energy transfer between ^{18}O- and ^{16}O-ethers during IRMP excitation, decreases the isotope selectivity. Practically, a lower pressure and a lower F value are used to obtain higher selectivities. The addition of a radical scavenger sometimes effectively prevents isotope-scrambling processes.

The material balance based on oxygen atoms is high enough for it to be concluded that the oxygen atoms in decomposed ethers are found mostly in CO, H_2CO, or CH_3CHO. However, approximately 10—30% of the oxygen-containing products have not been detected. This is probably because of the adsorption of H_2CO and CH_3CHO on the cell wall. It may, alternatively, be suggested that low-volatile oxygen-containing products, including a large number of carbon and oxygen atoms, are formed on the cell wall through the complicated reactions between the radicals and the starting ether.

From the observed results, the criteria for a suitable ether for oxygen-isotope separation by means of IRMPD are considered to be as follows. A higher selectivity of oxygen-isotopes in the cleavage of a C–O bond is, of course, the most important factor. Moreover, it is necessary for a good candidate (1) that the ether have a large Y_d, (2) that a highly selective decomposition process occur, and (3) that simple products be formed. On the basis of these factors, **1a** and **1f** may be said to be the most suitable ethers among the saturated open-chain ethers. In fact, the ^{18}O enrichment induced by a TEA CO_2 laser has been demonstrated in **1a**[5,6] and $(CF_3)_2O$.[1]

The ^{18}O enrichment by the IRMPD of **1a** and **1f** is now under investigation. We are also studying the IRMPD of cyclic ethers for the ^{18}O enrichment.

Thanks are due to Mr. Masahiro Toyoda, undergraduate student of Science University of Tokyo in 1982—1983, for his collaboration in the course of this experiment.

References

1) Part I: T. Majima, T. Igarashi, and S. Arai, *Nippon Kagaku Kaishi*, **1984**, 1490.

2) This work was partly reported at the 11th Int. Conf. on Photochem., Maryland (1983); T. Majima, S. Arai, T. Ishii, M. Toyoda, and T. Handa, Abstr. p. 27.

3) V. S. Letokhov, "Non-linear Laser Chemistry," Springer-Verlag, Berlin (1983).

4) W. C. Danen and J. C. Jang, "Laser-Induced Chemical Processes," ed by J. I. Steinfeld, Plenum Press, New York (1981), p. 45.

5) V. V. Vizhin, Y. N. Molin, A. K. Petrov, and A. R. Sorokin, *Appl. Phys.*, **17**, 385 (1978).

6) K. O. Kutschke, C. Willis, and P. A. Hackett, *J. Photochem.*, **21**, 207 (1983).

7) a) R. N. Rosenfeld, J. I. Brauman, J. R. Barker, and D. M. Golden, *J. Am. Chem. Soc.*, **99**, 8063 (1977); b) D. M. Brenner, *Chem. Phys. Lett.*, **57**, 357 (1978); c) P. Avouris, I. Y. Chan, and M. M. T. Loy, *J. Chem. Phys.*, **72**, 3522(1980); d) D. M. Brenner, *J. Phys. Chem.*, **86**, 41 (1982); e) F. Huisken, D. Krajnovich, Z. Zhang, Y. R. Shen, and Y. Y. Lee, *J. Chem. Phys.*, **78**, 3806 (1983).

8) D. Gutman, W. Braun, and W. Tsang, *J. Chem. Phys.*, **67**, 4291 (1977).

9) J. E. Kuder and D. R. Holcomb, *Chem. Phys. Lett.*, **86**, 11 (1982).

10) J. Kramer, *J. Phys. Chem.*, **86**, 26 (1982).

11) J. Kramer, *J. Photochem.*, **24**, 11 (1984).

12) W. E. Farneth and D. G. Johnson, *J. Am. Chem. Soc.*, **106**, 1875 (1984).

13) S. Ruhman, O. Anner, S. Gershuni, and Y. Haas, *Chem. Phys. Lett.*, **99**, 281 (1983); S. Ruhman, O. Anner, and Y. Haas, *J. Phys. Chem.*, **88**, 5162 (1984); Y. Haas, S. Ruhman, G. D. Greeblatt, and O. Anner, *J. Am. Chem. Soc.*, **107**, 5068 (1985).

14) a) S. Braslausky and J. Heicklen, *Chem. Rev.*, **77**, 473 (1977); b) C. Sonntag and H. -P. Schuchmann, *Adv. Photochem.*, **10**, 59 (1979).

15) G. R. Freeman, C. J. Danby, and C. Hinshelwood, *Proc. Roy. Soc. A*, **245**, 28 (1958); S. W. Benson and D. V. S. Jain, *J. Chem. Phys.*, **31**, 1008 (1959).

16) N. Bloembergen and E. Yablonovitch, *Phys. Today*, **31**, 23 (1978).

17) P. A. Schultz, A. S. Sudbo, D. J. Krajnovich, H. S. Kwok, Y. R. Shen, and Y. T. Lee, *Annu. Rev. Phys. Chem.*, **30**, 379 (1979).

18) M. Quack, *J. Chem. Phys.*, **69**, 1282 (1978); J. Troe, *ibid.*, **73**, 3205 (1980); A. C. Baldwin and J. R. Berker, *ibid.*, **74**, 3823 (1981).

19) W. E. Farneth and M. W. Thomsen, *J. Am. Chem. Soc.*, **105**, 1843 (1983).

20) F. D. Green, M. L. Savile, F. D. Osterholtz, H. H. Lau, W. N. Smith, and P. M. Zanet, *J. Org. Chem.*, **28**, 55 (1963).

21) S. W. Benson, "Thermochemical Kinetics." 2nd ed., Wiley, New York (1976).

22) B. S. Rabinovitch and D. W. Setser, *Adv. Photochem.*, **3**, 1 (1964).

23) D. L. Allara and R. Shaw, *J. Phys. Chem. Ref. Data*, **9**, 523 (1980); Th. Just, "Shock Waves in Chemistry," ed by A. Lifshitz, Marcel Dekker, New York (1981); G. B. Skinner, *ibid.;* N. C. Peterson, T. Ishii, and W. Braun, "Fast Reactions in Energetic Systems," ed by C. Capellos, R. F. Walker, D. Reidel Publishing, Dordrecht, Holland (1981), pp. 531—539.

24) R. F. C. Brown, "Pyrolytic Methods in Organic Chemistry," Academic Press, New York (1980).

25) J. A. Gray and D. W. G. Style, *Trans. Faraday Soc.*, **49**, 52 (1983).

26) H. Hershenson and S. W. Benson, *J. Chem. Phys.*, **37**, 1889 (1962).

27) T. Berces and A. F. Trotman-Dickerson, *J. Chem. Soc.*, **1961**, 348.

28) N. J. Daley and C. Wentrup, *Aust. J. Chem.*, **21**, 1535 (1968).

29) R. J. S. Morrison and E. R. Grant, *J. Chem. Phys.*, **71**, 3537 (1979); R. J. S. Morrison, R. F. Loring, R. L. Farley, and E. R. Grant, *ibid.*, **75**, 148 (1981).

30) R. T. Sanderson, "Chemical Bonds and Bond Energy," 2nd ed, Academic Press, New York (1976).